

A New Normalized Subband Adaptive Filter Algorithm with Individual Variable Step Sizes

Yi Yu¹ · Haiquan Zhao¹ · Badong Chen²

Received: 7 April 2015 / Revised: 20 June 2015 / Accepted: 22 June 2015 / Published online: 1 July 2015
© Springer Science+Business Media New York 2015

Abstract Proposed is a novel variable step size normalized subband adaptive filter algorithm, which assigns an individual step size for each subband by minimizing the mean square of the noise-free a posteriori subband error. Furthermore, a *noniterative shrinkage* method is used to recover the noise-free priori subband error from the noisy subband error signal. Simulation results using the colored input signals have demonstrated that the proposed algorithm not only has better tracking capability than the existing subband adaptive filter algorithms, but also exhibits lower steady-state error.

Keywords Normalized subband adaptive filter · Variable step size · Noniterative shrinkage method · Colored input signal

1 Introduction

In application fields of adaptive filtering algorithms such as system identification, noise cancellation, echo cancellation, and channel estimation, the widely used algorithm is the normalized least mean square (NLMS) due to its low computational complexity [7,9]. Compared to the conventional NLMS algorithm, the variable step size versions

✉ Haiquan Zhao
hqzhao@home.swjtu.edu.cn

Yi Yu
yuyi_xyuan@163.com

Badong Chen
chenbd@mail.xjtu.edu.cn

¹ School of Electrical Engineering, Southwest Jiaotong University, Chengdu, China

² School of Electronic and Information Engineering, Xi'an Jiaotong University, Xi'an, China

presented in [2, 3, 12, 16] offer the improved performance in terms of convergence rate and steady-state error. Nevertheless, these NLMS-type algorithms will suffer from slow convergence when the input signals are colored. Aiming to such input signals, the affine projection algorithm (APA) and its variants (e.g., see [13, 15] and the references therein) provide faster convergence rate than the NLMS algorithm. Because the APAs use the most recent input signal vectors to update the tap-weight vector, the NLMS uses only the current input signal vector. However, the APAs require large computational cost due to involving the matrix inversion operation in updating the tap-weight vector.

In a recent decade, in order to speed the convergence of filter for colored input signals, the subband adaptive filters (SAFs) have received great attention [4]. This is due to the fact that the SAF divides the colored input signal into almost mutually exclusive subband signals through analysis filters. Moreover, each subband input signal is approximate white. In [5], Lee and Gan proposed the normalized SAF (NSAF) algorithm based on the principle of minimum disturbance. This algorithm performs better than the NLMS in convergence rate for colored input signals, due to the inherent decorrelating property of SAF [6]. Also, the NSAF has almost the same computational complexity as the NLMS. Unfortunately, the performance of the original NSAF algorithm depends on the fixed step size that reflects a compromise between fast convergence rate and low steady-state error. To overcome this conflict, several variable step size NSAF algorithms have been proposed [1, 8, 10, 11]. In [1], a set-membership NSAF (SM-NSAF) algorithm was developed, whereas its convergence performance is sensitive to the selection of the error-bound parameter. The variable step size matrix NSAF (VSSM-NSAF) was presented in [8], which converged faster than the SM-NSAF. However, this algorithm still has large final estimation error. Following this approach, based on the same principle that minimizes the mean square deviation (MSD), two variable step size NSAF algorithms were proposed in [10] and [11], respectively. The difference is that the latter has a lower steady-state error than the former, since it uses an individual step size for each subband while the former uses a common step size for all subbands. Regrettably, both algorithms cannot track the changes in the unknown system.

In this paper, we propose a new variable step size NSAF algorithm, called NVSS-NSAF, based on the minimization of the mean square of the noise-free a posteriori subband error signals with respect to the step size. The proposed algorithm assigns an individual step size for each subband and uses the *noniterative shrinkage* method reported in [17] to estimate the noise-free a priori subband error signals.

2 The Original NSAF Algorithm

Consider the desired signal $d(n)$ which arises from the output end of the unknown system,

$$d(n) = \mathbf{u}^T(n)\mathbf{w}_o + \eta(n), \quad (1)$$

where $(\cdot)^T$ denotes the transpose of a vector, \mathbf{w}_o is the unknown M -dimensional vector that we wish to identify, $\mathbf{u}(n) = [u(n), u(n-1), \dots, u(n-M+1)]^T$ is the input signal vector, $\eta(n)$ is the system noise with zero-mean and variance σ_η^2 which is independent of $u(n)$.

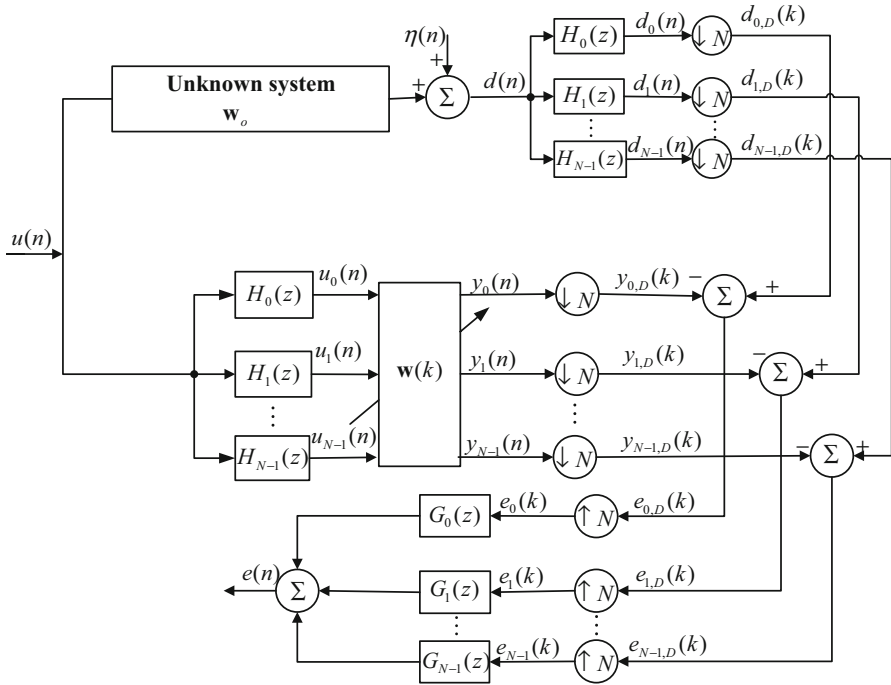


Fig. 1 Block diagram of multiband-structured SAF

Figure 1 shows the multiband structure of SAF, where N denotes the number of subbands. The signals $d(n)$ and $u(n)$ are partitioned into multiple subband signals by using analysis filters $\{H_i(z), i \in [0, N - 1]\}$, respectively. Then, the subband signals $y_i(n)$ and $d_i(n)$ for $i \in [0, N - 1]$ are critically decimated to yield $y_{i,D}(k)$ and $d_{i,D}(k)$, respectively. Here, n and k indicate the original sequences and the decimated sequences, respectively. The i th subband error signal $e_{i,D}(k)$ is defined as

$$e_{i,D}(k) = d_{i,D}(k) - y_{i,D}(k) = d_{i,D}(k) - \mathbf{u}_i^T(k)\mathbf{w}(k) \tag{2}$$

where $\mathbf{w}(k)$ is the tap-weight vector of filter, $\mathbf{u}_i(k) = [u_i(kN), u_i(kN - 1), \dots, u_i(kN - M + 1)]^T$, and $d_{i,D}(k) = d_i(kN)$.

As introduced in [5], the original NSAF algorithm for updating the tap-weight vector is expressed as

$$\mathbf{w}(k + 1) = \mathbf{w}(k) + \mu \sum_{i=0}^{N-1} \frac{\mathbf{u}_i(k)e_{i,D}(k)}{\mathbf{u}_i^T(k)\mathbf{u}_i(k)} \tag{3}$$

where μ is the step size.

3 Proposed Algorithm

3.1 Derivation of Algorithm

Replacing the fixed step size μ with the time-varying individual step sizes $\mu_i(k)$ for $i \in [0, N - 1]$, then (3) becomes

$$\mathbf{w}(k + 1) = \mathbf{w}(k) + \sum_{i=0}^{N-1} \mu_i(k) \frac{\mathbf{u}_i(k)e_{i,D}(k)}{\mathbf{u}_i^T(k)\mathbf{u}_i(k)}. \quad (4)$$

Before deriving $\mu_i(k)$, we define the noise-free a priori subband error and noise-free a posteriori subband error as follows:

$$\varepsilon_{i,a}(k) = \mathbf{u}_i^T(k) [\mathbf{w}_o - \mathbf{w}(k)], \quad (5)$$

$$\varepsilon_{i,p}(k) = \mathbf{u}_i^T(k) [\mathbf{w}_o - \mathbf{w}(k + 1)]. \quad (6)$$

Thus, (2) can also be expressed as

$$e_{i,D}(k) = \varepsilon_{i,a}(k) + \eta_{i,D}(k) \quad (7)$$

where $\eta_{i,D}(k)$ is the i th subband system noise, and its variance $\sigma_{\eta_{i,D}}^2$ can be computed by $\sigma_{\eta_{i,D}}^2 = \sigma_{\eta}^2/N$ [14].

Substituting (5)–(7) into (4), we have

$$\varepsilon_{i,p}(k) = [1 - \mu_i(k)] \varepsilon_{i,a}(k) - \mu_i(k) \eta_{i,D}(k) - \sum_{\substack{j=0 \\ j \neq i}}^{N-1} \mu_j(k) \frac{\mathbf{u}_i^T(k)\mathbf{u}_j(k)e_{j,D}(k)}{\mathbf{u}_j^T(k)\mathbf{u}_j(k)} \quad (8)$$

Applying the diagonal assumption that has been used to derive the original NSAF, i.e., $\mathbf{u}_i^T(k)\mathbf{u}_j(k) \approx 0, i \neq j$ [5], (8) can be simplified as

$$\varepsilon_{i,p}(k) = [1 - \mu_i(k)] \varepsilon_{i,a}(k) - \mu_i(k) \eta_{i,D}(k) \quad (9)$$

Taking the square and mathematical expectation of both sides of (9), we obtain

$$E \left[\varepsilon_{i,p}^2(k) \right] = [1 - \mu_i(k)]^2 E \left[\varepsilon_{i,a}^2(k) \right] + \mu_i^2(k) \sigma_{\eta_{i,D}}^2 \quad (10)$$

where $E[\cdot]$ denotes the mathematical expectation.

In order to obtain the optimum step size $\mu_i(k)$ at each iteration, we now solve the minimization problem of $E \left[\varepsilon_{i,p}^2(k) \right]$ with respect to $\mu_i(k)$. Taking the derivative of $E \left[\varepsilon_{i,p}^2(k) \right]$ with respect to $\mu_i(k)$ and setting it to zero, the step sizes $\mu_i(k)$ for $i \in [0, N - 1]$ are obtained as

$$\mu_i(k) = \frac{E \left[\varepsilon_{i,a}^2(k) \right]}{E \left[\varepsilon_{i,a}^2(k) \right] + \sigma_{\eta_{i,D}}^2} \tag{11}$$

Note that the step sizes $\mu_i(k)$ computed by (11) always lie in the range of (0, 1). This implies that the proposed algorithm is stable, based on the fact that the range of the step size in the original NSAF for stable convergence is $0 < \mu < 2$.

In practical applications, the statistical mean $E \left[\varepsilon_{i,a}^2(k) \right]$ is generally estimated by the time average of $\varepsilon_{i,a}^2(k)$, i.e.,

$$\sigma_{\varepsilon_{i,a}}^2(k) = \alpha \sigma_{\varepsilon_{i,a}}^2(k-1) + (1 - \alpha) \varepsilon_{i,a}^2(k) \tag{12}$$

where α is the forgetting factor, which is determined by $\alpha = 1 - N/\kappa M$, $\kappa \geq 1$ [8].

Now, the only thing that remains is to determine the noise-free a priori subband error $\varepsilon_{i,a}(k)$ in (12). Although $\varepsilon_{i,a}(k)$ is unknown in the entire adaptive process, it can be recovered from the subband error signal $e_{i,D}(k)$ by using the *noniterative shrinkage* method described in [3, 17], i.e.,

$$\varepsilon_{i,a}(k) = \text{sign} \left(e_{i,D}(k) \right) \max \left(|e_{i,D}(k)| - t_i, 0 \right) \tag{13}$$

where $\text{sign}(\cdot)$ denotes the sign function, and t_i is the threshold parameter. The method has obtained success in image denoising applications [17]. Based on our extensive simulation results, it is found that $t_i = \sqrt{\lambda \sigma_{\eta_{i,D}}^2}$ with $\lambda = 3\text{--}5$ can yield good results. Hence, the proposed NVSS–NSAF algorithm is summarized in Table 1.

Table 1 Proposed NVSS–NSAF algorithm

Initialization	$\mathbf{w}(0) = 0, \quad \sigma_{\varepsilon_{i,a}}^2(0) = 0$
Parameters	$t_i = \sqrt{\lambda \sigma_{\eta}^2} / N$, threshold parameter with $\lambda = 3\text{--}5$ $\alpha = 1 - N/\kappa M$, forgetting factor with $\kappa > 1$
Adaptive process	for $i \in [0, N - 1]$ $e_{i,D}(k) = d_{i,D}(k) - \mathbf{u}_i^T(k) \mathbf{w}(k)$ $\varepsilon_{i,a}(k) = \text{sign} \left(e_{i,D}(k) \right) \max \left(e_{i,D}(k) - t_i, 0 \right)$ $\sigma_{\varepsilon_{i,a}}^2(k) = \alpha \sigma_{\varepsilon_{i,a}}^2(k-1) + (1 - \alpha) \varepsilon_{i,a}^2(k)$ $\mu_i(k) = \frac{\sigma_{\varepsilon_{i,a}}^2(k)}{\sigma_{\varepsilon_{i,a}}^2(k) + \sigma_{\eta_{i,D}}^2}$ end $\mathbf{w}(k+1) = \mathbf{w}(k) + \sum_{i=0}^{N-1} \mu_i(k) \frac{\mathbf{u}_i(k) e_{i,D}(k)}{\mathbf{u}_i^T(k) \mathbf{u}_i(k)}$

3.2 Convergence of Algorithm

In this section, the convergence of the proposed algorithm is analyzed based on the mean square deviation (MSD) defined by

$$m(k) = E \left[\|\boldsymbol{\theta}(k)\|^2 \right] \triangleq E \left[\|\mathbf{w}_o - \mathbf{w}(k)\|^2 \right] \quad (14)$$

where $\|\cdot\|$ denotes the Euclidean norm of a vector.

Subtracting (4) from \mathbf{w}_o , taking the squared Euclidean norm of both sides, and then applying (5), we have

$$\|\boldsymbol{\theta}(k+1)\|^2 = \|\boldsymbol{\theta}(k)\|^2 - 2 \sum_{i=0}^{N-1} \mu_i(k) \frac{\varepsilon_{i,a}(k)e_{i,D}(k)}{\mathbf{u}_i^T(k)\mathbf{u}_i(k)} + \sum_{i=0}^{N-1} \mu_i^2(k) \frac{e_{i,D}^2(k)}{\mathbf{u}_i^T(k)\mathbf{u}_i(k)} \quad (15)$$

where we again use the diagonal assumption [5].

From (11), one can know that $\mu_i(k)$ for $i \in [0, N-1]$ are deterministic in nature; thus, we can express the mathematical expectation of both sides of (15) as

$$m(k+1) = m(k) - 2 \sum_{i=0}^{N-1} \mu_i(k) E \left[\frac{\varepsilon_{i,a}(k)e_{i,D}(k)}{\mathbf{u}_i^T(k)\mathbf{u}_i(k)} \right] + \sum_{i=0}^{N-1} \mu_i^2(k) E \left[\frac{e_{i,D}^2(k)}{\mathbf{u}_i^T(k)\mathbf{u}_i(k)} \right]. \quad (16)$$

For a high-order adaptive filter, the fluctuation of $\|\mathbf{u}_i(k)\|^2$ from one iteration to the next can be assumed to be small enough, so that (16) becomes

$$m(k+1) - m(k) = - \sum_{i=0}^{N-1} \mu_i(k) \frac{2E \left[\varepsilon_{i,a}(k)e_{i,D}(k) \right] - \mu_i(k)E \left[e_{i,D}^2(k) \right]}{E \left[\mathbf{u}_i^T(k)\mathbf{u}_i(k) \right]}. \quad (17)$$

Substituting (7) and (11) into (17), and using the common assumption that $\varepsilon_{i,a}(k)$ is independent of $\eta_{i,D}(k)$ [8, 14], we get

$$m(k+1) - m(k) = - \sum_{i=0}^{N-1} \frac{\left(E \left[\varepsilon_{i,a}^2(k) \right] \right)^2}{\left(E \left[\varepsilon_{i,a}^2(k) \right] + \sigma_{\eta_{i,D}}^2 \right) E \left[\mathbf{u}_i^T(k)\mathbf{u}_i(k) \right]} \leq 0. \quad (18)$$

It is clear that $m(k)$ is nonincreasing, which implies that the proposed algorithm is convergent as k increases. Also, the equality in (18) holds if and only if the algorithm has gone into the steady state, i.e., $m(k+1) = m(k)$ as $k \rightarrow \infty$. Hence, in this case, we obtain

$$E \left[\varepsilon_{i,a}^2(\infty) \right] = 0, \quad i \in [0, N-1]. \quad (19)$$

Based on the fact that each subband input is close to a white signal [8, 10], (19) can be simplified as $E \left[\varepsilon_{i,a}^2(\infty) \right] \approx m(\infty)\sigma_{u_i}^2 = 0$, which implies $m(\infty) = E \left[\|\boldsymbol{\theta}(\infty)\|^2 \right]$

= 0. As a result, the proposed algorithm can theoretically converge to the optimal solution \mathbf{w}_o in the mean square sense.

4 Simulation Results

In order to assess the algorithm performance, the Monte Carlo (MC) simulations (average of 50 independent runs) are performed in the system identification scenarios. In our simulations, the unknown vector \mathbf{w}_o is a room acoustic impulse response with $M = 512$ taps. Also, to show the tracking capability of the algorithm, the unknown vector is changed as $-\mathbf{w}_o$ at the 8×10^4 th input samples. The colored input signal $u(n)$ is generated by filtering a zero-mean white Gaussian signal through a first-order system $\phi_1(z) = 1/(1 - 0.9z^{-1})$ or a second-order system $\phi_2(z) = 1/(1 - 1.6z^{-1} + 0.81z^{-2})$ [10]. The background noise $\eta(n)$ is a white Gaussian signal with a signal-to-noise ratio (SNR) of 30 dB, unless otherwise specified. Here, we assume that the variance of the system noise, σ_η^2 , is known, because it can be easily estimated online [8, 10, 11]. The cosine modulated filter bank is used in all the SAF algorithms [4]. The normalized MSD (NMSD), $10 \log_{10} [\|\mathbf{w}_o - \mathbf{w}(k)\|_2^2 / \|\mathbf{w}_o\|_2^2]$, is used to measure the performance of the algorithms.

This work first examines the performance of the proposed algorithm using different numbers of subbands (i.e., $N = 2, 4$, and 8), as shown in Fig. 2. The colored input signal is generated by ϕ_1 . As expected, the convergence rate of a large number of subbands (e.g., $N = 8$) is faster than that of a small one (e.g., $N = 2$). The reason is behind this phenomenon is that each subband input signal is closer to a white signal for a larger number of subbands. However, this phenomenon will not be obvious when the number of subbands is larger than a certain value (in this case is 4). Besides,

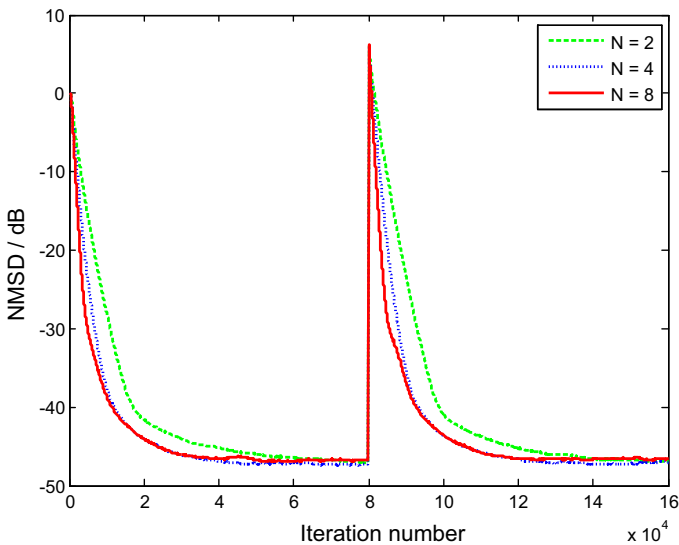


Fig. 2 NMSD curves of the NVSS-NSAF with $N = 2, 4$, and 8

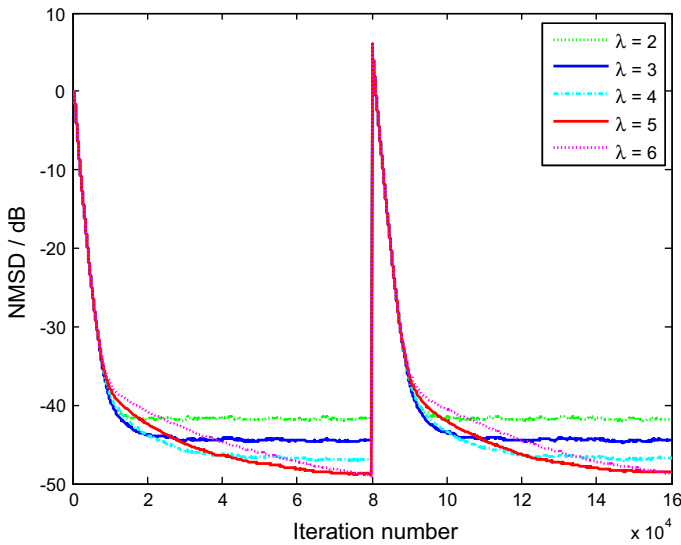


Fig. 3 NMSD curves of the NVSS-NSAF for different values of λ

increasing the number of subbands also means increased computational complexity. Thus, a proper selection of N relies on a trade-off between convergence rate and computational complexity. Based on this principle, the number of subbands is chosen as $N = 4$ in the following simulations.

Since the proposed algorithm uses the *noniterative shrinkage* method to estimate $\varepsilon_{i,a}(k)$, i.e., (13), the parameter λ must be selected properly. Figure 3 investigates the effect of λ on the performance of the proposed algorithm, where the input signal is the same as Fig. 2. As can be seen, a suitable range of λ is $3 \leq \lambda \leq 5$, because the proposed algorithm obtains a good balance between convergence rate and steady-state error.

Finally, the performance of the proposed NVSS-NSAF algorithm is compared to that of the NSAF algorithm with two fixed step sizes, the VSSM-NSAF algorithm [8] and the VSS-NSAF algorithm with two values of β [11], as shown in Figs. 4 and 5. In Fig. 4a, b, the colored input signals are generated by ϕ_1 and ϕ_2 , respectively, and SNR = 30dB. To fairly compare the algorithms, the number of subbands $N = 4$ is used in all the algorithms, and the parameters of the algorithms in [8] and [11] are chosen according to the recommended values in the literatures. It is clear that variable step size algorithms (e.g., VSSM-NSAF, VSS-NSAF, and NVSS-NSAF) improve the performance of filter in terms of convergence rate and steady-state error, as compared to the NSAF with the fixed step size. However, among these variable step size algorithms, the VSSM-NSAF in [8] has the largest steady-state error, and the NVSS-NSAF has the lowest steady-state error. Choosing a proper value of β , the VSS-NSAF in [11] can obtain the same convergence rate or steady-state error as the NVSS-NSAF, but it sacrifices the steady-state error or convergence rate. Besides, the VSS-NSAF in [11] has no tracking capability when the unknown system suddenly changes. Figure 5 describes the NMSD results of these SAFs for SNR = 20 dB,

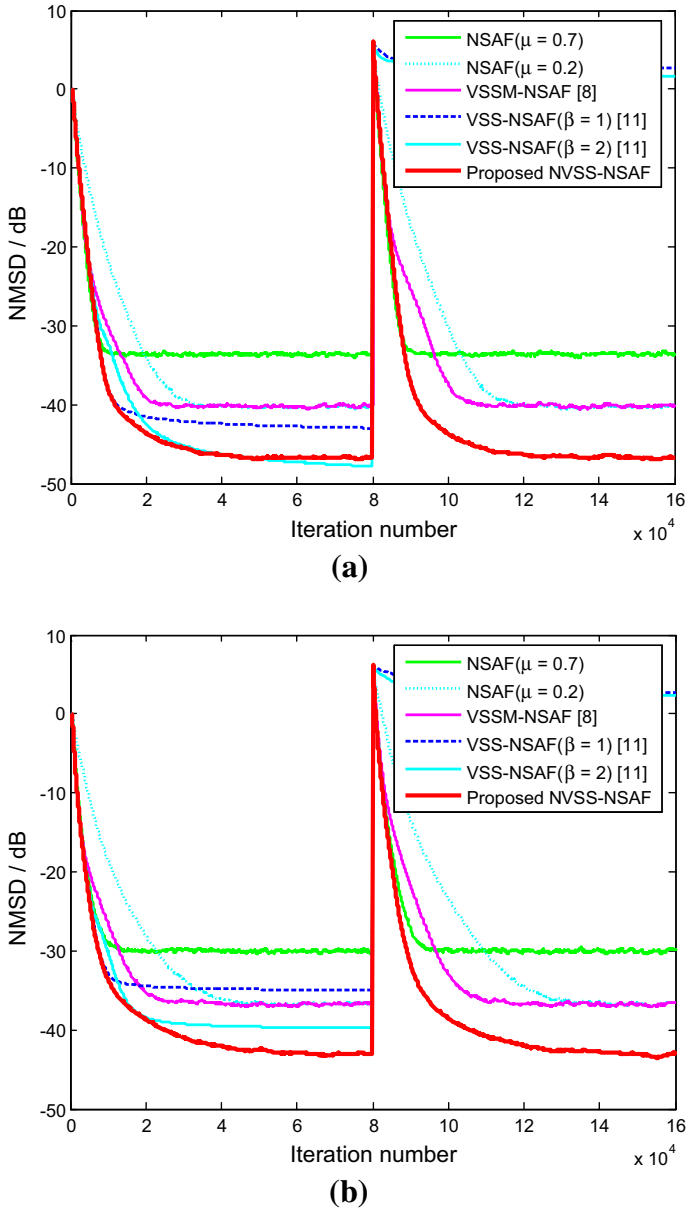
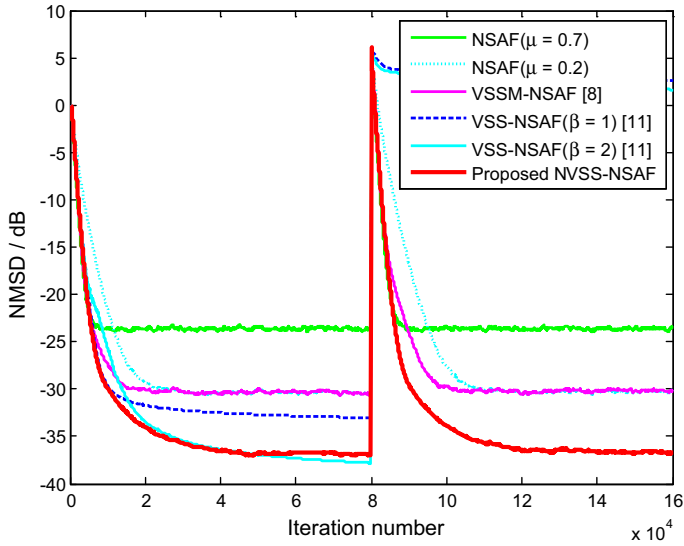
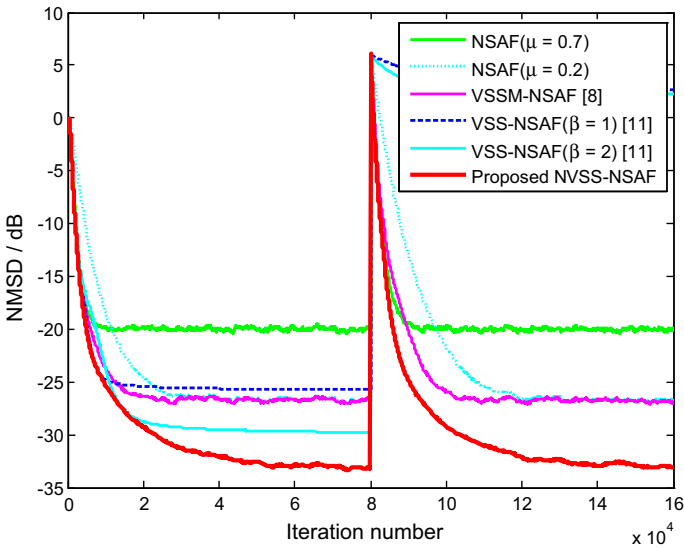


Fig. 4 NMSD curves of various SAF algorithms with SNR = 30 dB. **a** The colored input is generated by ϕ_1 . **b** The colored input is generated by ϕ_2 . NSAF: $\mu = 0.7$ and $\mu = 0.2$; VSSM-NSAF: $\kappa = 6$ [8]; VSS-NSAF: $tr\{\mathbf{P}(0)\} = 100$ and $\beta = 1, 2$ [11]; proposed NVSS-NSAF: $\kappa = 1, \lambda = 4$ (Color figure online)

using the colored input signals generated by ϕ_1 and ϕ_2 . As one can see, the proposed algorithm still outperforms the other algorithms in terms of convergence rate, steady-state error, and tracking capability. Moreover, one can also observe from Figs. 4 and 5



(a)



(b)

Fig. 5 NMSD curves of various SAF algorithms with SNR = 20 dB. **a** The colored input is generated by ϕ_1 . **b** The colored input is generated by ϕ_2 . The choices of the algorithms parameters are the same as Fig. 4 (Color figure online)

that the steady-state errors of these algorithms using the same input signal increase as the SNR decreases.

5 Conclusions

In this study, we derived the NVSS–NSAF algorithm by solving the minimization problem of the mean square of the noise-free a posteriori subband error with respect to the step size. The proposed algorithm uses an individual step size for each subband. In order to recover the noise-free a priori subband error from the noisy subband error signal, a *noniterative shrinkage* method was employed. Compared to the conventional NSAF, VSSM–NSAF in [8], and VSS–NSAF in [11] algorithms, the proposed algorithm obtains good performance in terms of the tracking capability and steady-state error.

Acknowledgments This work was supported by National Science Foundation of P.R. China (Grants: 61271340 and 61433011), the Sichuan Provincial Youth Science and Technology Fund (Grant: 2012JQ0046), and the Fundamental Research Funds for the Central Universities (Grant: SWJTU12CX026).

References

1. M.S.E. Abadi, J.H. Husøy, Selective partial update and set-membership subband adaptive filters. *Signal Process.* **88**(10), 2463–2471 (2008)
2. J. Benesty, H. Rey, L.R. Vega, S. Tressens, A nonparametric VSS NLMS algorithm. *IEEE Signal Process. Lett.* **13**(10), 581–584 (2006)
3. M.Z.A. Bhotto, A. Antoniou, A family of shrinkage adaptive filtering algorithms. *IEEE Trans. Signal Process.* **61**(7), 1689–1697 (2013)
4. K.A. Lee, W.S. Gan, S.M. Kuo, *Subband Adaptive Filtering: Theory and Implementation* (Wiley, Hoboken, 2009)
5. K.A. Lee, W.S. Gan, Improving convergence of the NLMS algorithm using constrained subband updates. *IEEE Signal Process. Lett.* **11**(9), 736–739 (2004)
6. K.A. Lee, W.S. Gan, Inherent decorrelating and least perturbation properties of the normalized subband adaptive filter. *IEEE Trans. Signal Process.* **54**(11), 4475–4480 (2006)
7. U. Mahbub, S.A. Fattah, A single-channel acoustic echo cancellation scheme using gradient-based adaptive filtering. *Circuits Syst. Signal Process.* **33**(5), 1541–1572 (2014)
8. J. Ni, F. Li, A variable step-size matrix normalized subband adaptive filter. *IEEE Trans. Audio Speech Lang. Process.* **18**(6), 1290–1299 (2010)
9. A.H. Sayed, *Adaptive Filters* (Wiley, New York, 2008)
10. J.W. Shin, N.W. Kong, P.G. Park, Normalised subband adaptive filter with variable step size. *Electron. Lett.* **48**(4), 204–206 (2012)
11. J.H. Seo, P.G. Park, Variable individual step-size subband adaptive filtering algorithm. *Electron. Lett.* **50**(3), 177–178 (2014)
12. Y. Yu, H. Zhao, An improved variable step-size NLMS algorithm based on a Versiera function, in *IEEE International Conference on Signal Processing, Communication and Computing* (China, 2013), pp. 1–4
13. Y. Yu, H. Zhao, Memory proportionate APSA with individual activation factors for highly sparse system identification in impulsive noise environment, in *IEEE International Conference on Wireless Communications and Signal Processing (WCSP)*, (China, 2014), pp. 1–6
14. W. Yin, A.S. Mehr, Stochastic analysis of the normalized subband adaptive filter algorithm. *IEEE Trans. Circuits Syst. I Reg. Pap.* **58**(5), 1020–1033 (2011)
15. H. Zhao, Y. Yu, S. Gao, X. Zeng, Memory proportionate APA with individual activation factors for acoustic echo cancellation. *IEEE/ACM Trans. Audio Speech Lang. Process.* **22**(6), 1047–1055 (2014)

16. S. Zhao, D.L. Jones, S. Khoo, Z. Man, New variable step-sizes minimizing mean-square deviation for the LMS-type algorithms. *Circuits Syst. Signal Process.* **33**(7), 2251–2265 (2014)
17. M. Zibulevsky, M. Elad, L_1 – L_2 optimization in signal and image processing. *IEEE Signal Process. Mag.* **27**(3), 76–88 (2010)